HELDA
HELSINGIN YLIOPISTO
HELSINGFORS UNIVERSITET
UNIVERSITY OF HELSINKI

UNIVERSITY OF HELSINKI

https://helda.helsinki.fi

The H-1 and C-13 chemical shifts of 5-5 lignin model dimers : An evaluation of DFT functionals

Nguyen, Thien T.

2021-02-15

Nguyen , T T , Le , P Q , Helminen , J & Sipilä , J 2021 , ' The H-1 and C-13 chemical shifts of 5-5 lignin model dimers : An evaluation of DFT functionals ' , Journal of Molecular Structure , vol. 1226 , 129300 . https://doi.org/10.1016/j.molstruc.2020.129300

http://hdl.handle.net/10138/354575
https://doi.org/10.1016/j.molstruc.2020.129300

cc_by_nc_nd
acceptedVersion

Downloaded from Helda, University of Helsinki institutional repository.

This is an electronic reprint of the original article.

This reprint may differ from the original in pagination and typographic detail.

Please cite the original version.

The ^{1}H and ^{13}C chemical shifts of 5-5 lignin model dimers: an evaluation of DFT functionals

Thien T. Nguyen,[1,2*] Phong Q. Le,[3] Jussi Helminen,[4] Jussi Sipilä[4]

[1] Institute of Research and Development, Duy Tan University, Da Nang 550000, Vietnam

[2] Faculty of Natural Science, Duy Tan University, Da Nang 550000, Vietnam

[3] School of Biotechnology, International University, Vietnam National University, Ho Chi Minh City 700000, Vietnam

[4] Department of Chemistry, University of Helsinki, A.I. Virtasen aukio 1, Helsinki FI-00014 Helsinki, Finland

*****Corresponding Author: nguyentrongthien@duytan.edu.vn

Abstract

The calculations of ^{1}H and ^{13}C NMR chemical shifts were performed on three 5-5 lignin dimers, prominent substructures in softwood lignins, to compare with experimental data. Initially, 10 DFT functionals (B3LYP, B3PW91, BPV86, CAM-B3LYP, HCTH, HSEH1PBE, mPW1PW91, PBEPBE, TPSSTPSS, and ωB97XD) combined with the gauge-including atomic orbital (GIAO) method and basic set 6-31G(d,p) were tested on 3,3'-(6,6'-dihydroxy-5,5'-dimethoxy-[1,1'-biphenyl]-3,3'-diyl)dipropionic acid (**1**), efficiently synthesized from ferulic acid. HSEH1PBE, mPW1PW91, and ωB97XD were found to be the three best performing functionals with strong correlations ($r^2 \geq 0.9988$) and low errors (CMAEs $\leq$ 0.0611 ppm for ^{1}H and CMAEs $\leq$ 1.19 ppm for ^{13}C). These functionals were also well-performed for the ^{1}H and ^{13}C shift calculations of dimers 3,3'-dimethoxy-5,5'-dimethyl-[1,1'-biphenyl]-2,2'-diol (**2**) and 5,5'-diallyl-3,3'-dimethoxy-[1,1'-biphenyl]-2,2'-diol (**3)**. Overall, the ωB97XD functional consistently provided the calculated ^{1}H and ^{13}C chemical shifts with a high level of accuracy.

Keywords: 5-5 lignin model dimer, oxidative coupling, NMR chemical shift, DFT functionals

Introduction

Lignin, a potential feedstock for sustainable production of fuels, chemicals, and materials, comprising about one third of the dry weight of wood materials is a class of heterogenic aromatic polymers formed in a random dehydrogenative polymerization of three primary precursors (*p*-coumaryl, coniferyl, and sinapyl alcohols, Figure 1A) during plant cell wall biosynthesis [1][2][3][4]. Lignin model dimers, such as β-5, β-O-4, and 5-5 dimers, are prominent substructures found in lignin structure (Figure 1B and 1C). These compounds are interested by their potentials for studying lignin pyrolysis,[5] the ligninolytic capabilities of enzymes,[6] the dimer degradation using bacterial cultures,[7] oxidative cleavage,[8] and hydrodeoxygenation [9][10].

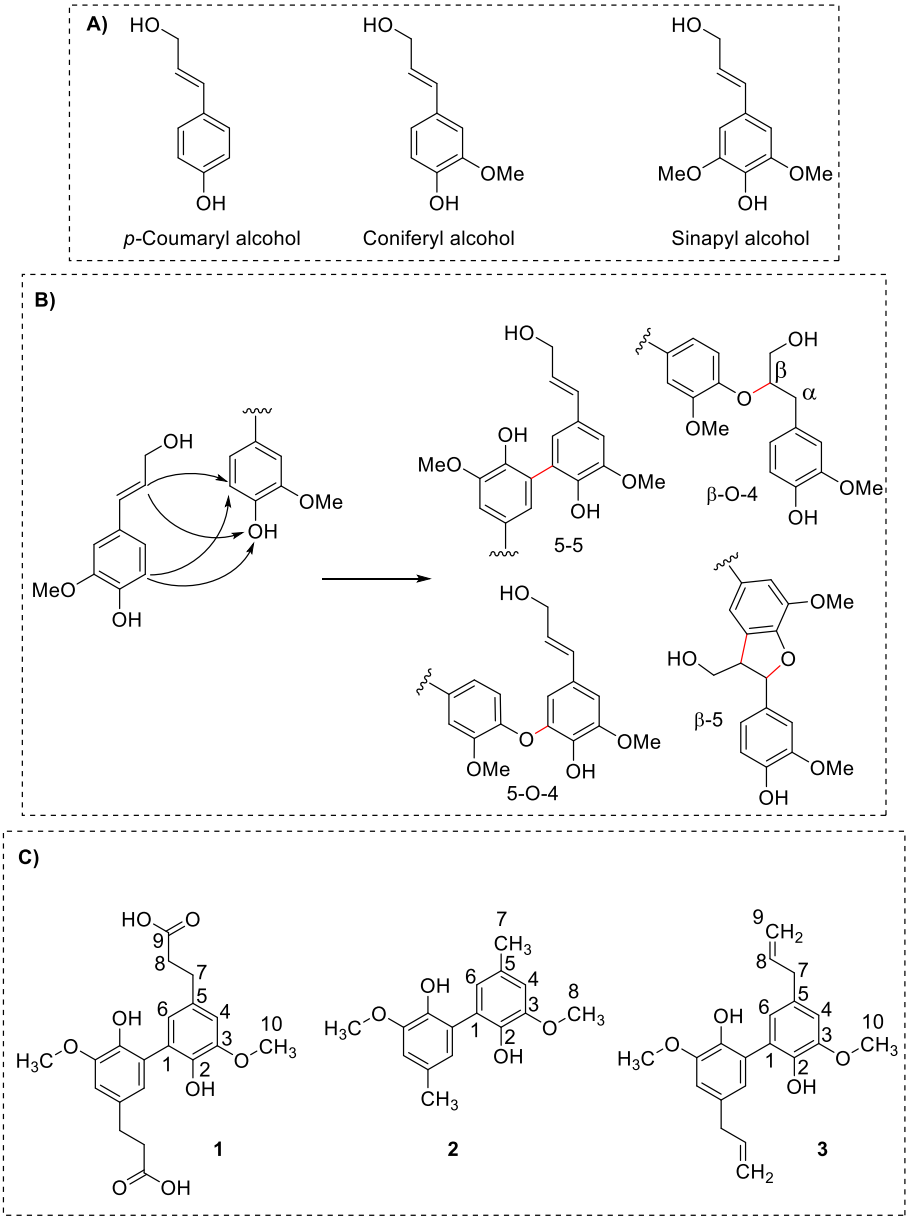

Figure 1. **A)** Lignin monomers; **B)** Ligninfication; **C)** 5-5 Lignin model dimers with number labels

The combination of experimental and computational nuclear magnetic resonance (NMR) techniques has been a strong tool for providing the structural information of lignin monomers, dimers, and oligomers, which can support the difficult assignments and the confirmation of their structures and provide valuable insights into the substructures of lignin biopolymers [11][12][13]. The gauge-including atomic orbitals (GIAO)/density functional theory (DFT) method are generally accepted as a standard method in computing shielding constants due to its reliability and applicability [14][15][16]. The accuracy of calculated chemical shifts typically depends on an appropriate combination of exchange-correlation functionals and basis sets [17]. Even though an experimental NMR database of lignin dimers is available,[18] there have been just few reports on comparing calculated NMR spectra with the available data for lignin monomers and dimers. Herein, this present study evaluated 10 DFT functionals including B3LYP (Becke's 3-parameter hybrid functional [19] using B exchange [20] and LYP correlation),[21][22] B3PW91 (Perdew

and Wang's 1991 gradient-corrected correlation functional),[23][24] BPV86 (Perdew's 1986 functional),[19][25][26] CAM-B3LYP (Handy and co-workers' long-range corrected version of B3LYP using the Coulomb-attenuating method),[27] HCTH (Hamprecht-Cohen-Tozer-Handy GGA functional),[28][29][30] HSEH1PBE (The exchange part of the screened Coulomb potential of Heyd, Scuseria, and Ernzerhof),[31][32] mPW1PW91 (mPW exchange and PW91 correlation),[33][34] PBEPBE (The functional of Perdew, Burke, and Ernzerhof),[35] TPSSTPSS (The exchange component of the Tao-Perdew-Staroverov-Scuseria),[36][37] and ωB97XD (Head-Gordon and coworkers' dispersion corrected long-range corrected hybrid functional)[38][39] on the ^{1}H and ^{13}C NMR shift calculations of 5-5 lignin model dimers (Figure 1C). Initially, the 10 cited functionals coupled with 6-31G(d,p) basis set [40] were tested on compound **1**, which was efficiently prepared by a two-stepped synthesis from ferulic acid. The statistical parameters including the corrected mean absolute error (CMAE), corrected root-mean-squared error (CRMSE), and the coefficient of determination (r^2) were employed for selecting the three best performing functionals for each nucleus, which were used for the ^{1}H and ^{13}C chemical shift calculations of similar model dimers **2** and **3** (Figure 1C).

Computational methods

All calculations were performed using the Gaussian09 [41]. Geometry optimizations of dimers **1**, **2**, and **3** were performed at the CAM-B3LYP/6-31G(d,p) level. The solvent effects of dimethylsulfoxide (DMSO) or chloroform ($CHCl_3$) were incorporated during the optimizations using the integral equation formalism variant of the polarized continuum model (IEFPCM) [42][43]. Subsequent frequency calculations ensured that a potential energy surface (PES) local minimum was attained during the energy minimization. Cartesian coordinates of the resulting structures are given in the Supporting Information.

Single-point NMR GIAO calculations were carried out at DFT level with IEFPCM method using the permittivity constants for dimethylsulfoxide or chloroform for both carbon and proton. The following 10 common functionals used for the NMR shielding constant calculations were considered: B3LYP, B3PW91, BPV86, CAM-B3LYP, HCTH, HSEH1PBE, mPW1PW91, PBEPBE, TPSSTPSS, and ωB97XD. The GIAO NMR results were observed and extracted using GaussView05. Each optimized structure of dimers and tetramethylsilane were used for computing the corresponding isotropic shielding constants σ_{cal} and σ_{TMS} using all the 10 cited functionals coupled with basis set 6-31G(d,p), the chemical shifts (δ_{cal}) were obtained using Equation 1. For both the ^{1}H and ^{13}C NMR calculations, an average of values of equivalents atoms was assumed. To reduce the systematic error of the calculations, the linear regression analysis of the calculated chemical shifts versus the experimental ones (δ_{exp}) (Equation 2) was performed and the scaled chemical shifts (δ_{scal}) were computed according to Equation 3. The results were evaluated using the corrected mean absolute error (CMAE/ppm, Equation 4); the corrected root mean squared error (CRMSE/ppm, Equation 5); and the coefficient of determination (r^2). The error calculations and linear correlations were performed using Microsoft Excel 2013.

$$\delta_{cal} = \sigma_{TMS} - \sigma_{cal} \quad (1)$$

$$\delta_{cal} = a\delta_{exp} + b \quad (2)$$

$$\delta_{scal} = (\delta_{cal} - b)/a \quad (3)$$

$$\mathrm{CMAE} = \sum_{1}^{n} \left| \delta_{scal} - \delta_{exp} \right| / n \quad (4)$$

$$\mathrm{CRMSE} = \sqrt{\sum_{1}^{n} (\delta_{scal} - \delta_{exp})^2 / n} \quad (5)$$

Figure 1C shows the numbered dimers used for the proton and carbon atoms in this study. Due to the axial symmetry of 5-5 dimers **1**, **2**, and **3**, only one side of the structures was labeled. The 5-5 dimers have phenolic and carboxylic protons which are typically not appeared in the NMR spectra due to rapid exchanges in DMSO-d_6 or $CDCl_3$ solvent. Therefore, this work excluded these protons in the calculations. The experimental ^{1}H and ^{13}C NMR spectra of **1** are available in Supplementary Information and those of **2** [44][45] and **3** [46][47] have been reported.

Results and Discussion

*Synthesis of dimer **1***

5-5 lignin model dimer **1** was prepared using a two-step sequence from ferulic acid using hydrogenation and oxidation reactions (Scheme 1). In the first step, ferulic acid was hydrogenated in two hours at room temperature using 10% Pd/C as the catalyst to produce dihydroferulic acid in a yellow solid form. In the second step, treatment of dihydroferulic acid with iodine in a basic condition (0.5 M NaOH aqueous solution) produced 5-5 lignin model dimer **1** as the oxidative coupling product in 72% yield.

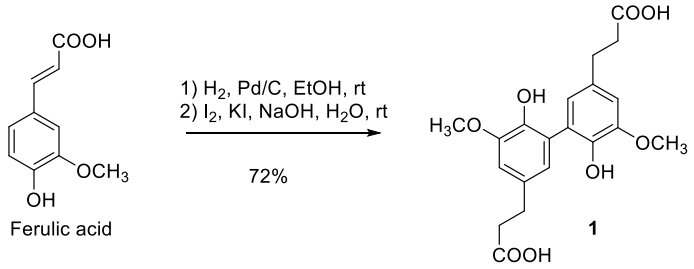

Scheme 1. Preparation of 5-5' lignin model dimer **1** from ferulic acid

The structure of lignin model dimer **1** ($C_{20}H_{22}O_8$; MW = 390.4) contains 14 methylene and methyl protons and 4 aromatic protons. Among 20 C atoms, 14 are sp^2-hybridized and 6 are sp^3-hybridized. Due to the free rotation about the biphenyl linkage, the ^{1}H and ^{13}C NMR spectra recorded at 298 K in DMSO shows 5 ^{1}H peaks and 10 ^{13}C peaks, as presented in Table 1. In those spectra, chemical shifts at low field area were assigned to aromatic protons (**H4** and **H6**) and sp^2-hybridized carbons (**C1-6** and **C9**), and those at high field area were belongs to aliphatic protons (**H7**, **H8**, and **H10**) and sp^3-hybridized carbons **(C7**, **C8**, and **C10)**. The coupling constant value of 2.1 Hz between the two aromatic protons indicated an *ortho* relationship.

The evaluation of 10 DFT functionals

Dimer **1** served as a representative 5-5 lignin model compound for evaluating the accuracy of ^{1}H and ^{13}C NMR calculations. 10 Functionals were evaluated, and the results were showed in Table 1 and 2. In these Tables, the functionals were sorted alphabetically by name. The same procedure was used for computing the chemical shifts of the reference trimethylsilane (TMS). To better represent the atoms in the same chemical environment, the mean value was considered. The

statistical parameters including CMAE, CRMSE, and r^2 were employed for quantifying the performance of each functional. The smaller values of CMAE and CRMSE indicate smaller errors and the larger value of r^2 means a stronger correlation between theoretical and experimental data. We based the discussion using these parameters in order to select the most accurate functionals.

Table 1 shows the experimental and calculated ^{1}H chemical shifts using 10 different DFT functionals coupled with 6-31G(d,p) basis set and Figure 2 illustrates the CMAE and CRMSE error bars. Overall, the correlation coefficients and error results indicate that the calculations provided a qualitatively accurate description of the ^{1}H NMR chemical shifts of compound **1**. The CMAE and CRMSE values were in the ranges of 0.0519 to 0.106 ppm and 0.0534 to 0.111 ppm, respectively. The coefficients of determination (r^2) were above 0.9964 for all tested functionals. Methylene protons **H7** were observed with the noticeable deviations ranged from 0.0715 to 0.166 ppm (Figure 3). The deviations of aromatic protons **H4** and **H6** were in the range of 0.0493 to 0.113 ppm. The three best performers with strong correlations and low errors for ^{1}H calculations were HSEH1PBE (CMAE = 0.0611 ppm, CRMSE = 0.0643 ppm, and r^2 = 0.9988), mPW1PW91 (CMAE = 0.0610 ppm, CRMSE = 0.0650 ppm, and r^2 = 0.9988), and ωB97XD (CMAE = 0.0519 ppm, CRMSE = 0.0534 ppm, and r^2 = 0.9992).

Table 1. The ^{1}H NMR chemical shifts of **1** calculated using 10 functionals coupled with 6-31G(d,p) basis set in DMSO solvent. All chemical shifts, CMAEs, and CRMSEs are in ppm.

	^{1}H NMR Chemical shifts (**1**, DMSO)					Statistical parameters		
	H4	**H6**	**H7**	**H8**	**H10**	CMAE	CRMSE	r^2
δ_{exp}	6.56	6.78	2.74	2.49	3.79			
B3LYP	6.48	6.84	2.62	2.55	3.86	0.0794	0.0816	0.9981
B3PW91	6.49	6.84	2.64	2.57	3.82	0.0688	0.0723	0.9985
BPV86	6.46	6.85	2.57	2.58	3.89	0.106	0.111	0.9964
CAMB3LYP	6.49	6.84	2.64	2.55	3.84	0.0674	0.0692	0.9986
HCTH	6.47	6.85	2.60	2.57	3.87	0.0936	0.0966	0.9973
HSEH1PBE*	**6.50**	**6.83**	**2.65**	**2.56**	**3.82**	**0.0611**	**0.0643**	**0.9988**
mPW1PW91*	**6.50**	**6.84**	**2.65**	**2.56**	**3.81**	**0.0610**	**0.0650**	**0.9988**
PBEPBE	6.46	6.86	2.58	2.58	3.88	0.104	0.108	0.9966
TPSSTPSS	6.45	6.87	2.60	2.56	3.89	0.102	0.105	0.9968
w*B97XD	**6.50**	**6.83**	**2.67**	**2.54**	**3.82**	**0.0519**	**0.0534**	**0.9992**

*The three functionals with lowest errors are in bold.

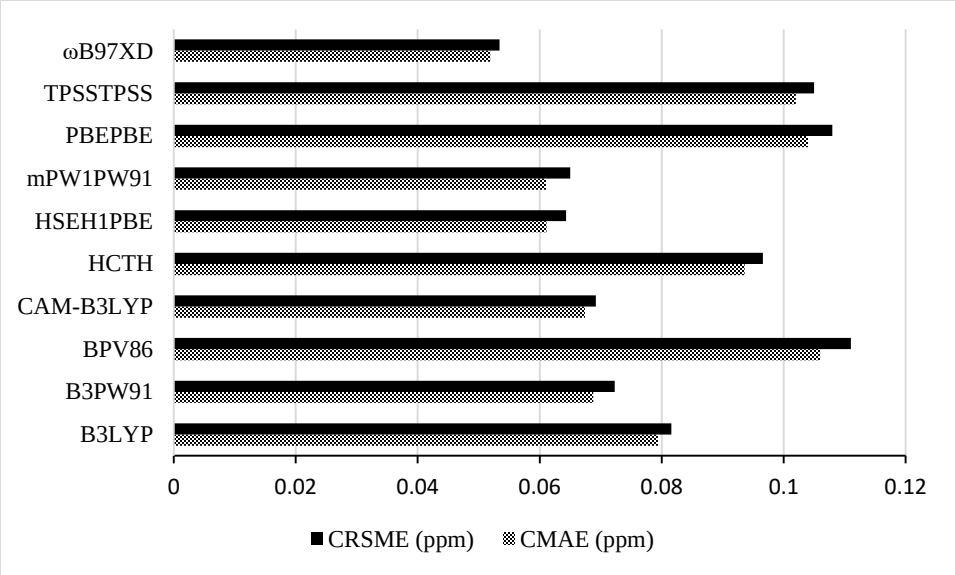

Figure 2. CMAE and CRSME values for the ^{1}H chemical shift calculations of dimer **1**

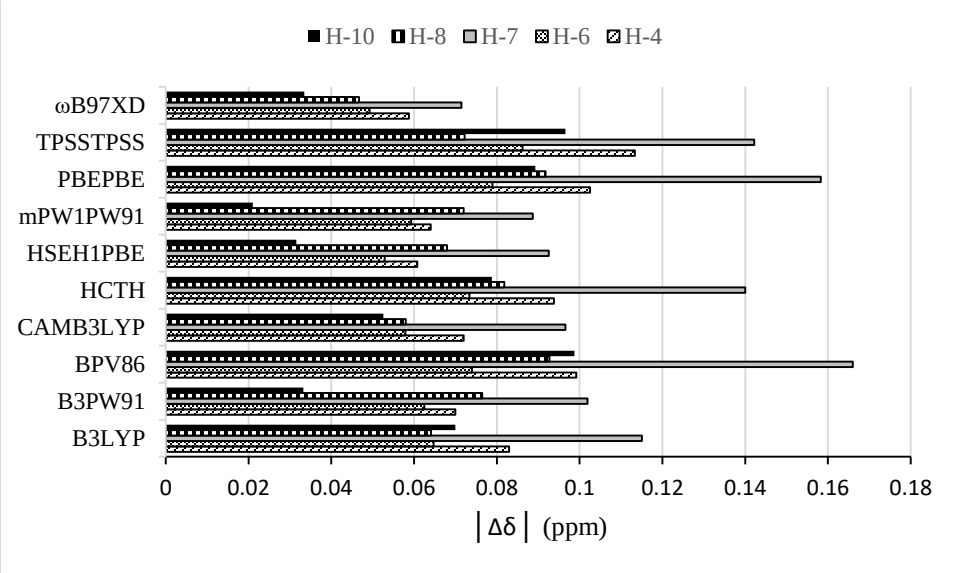

Figure 3. Absolute deviations of for the ^{1}H chemical shift calculations of dimer **1**

The calculated ^{13}C NMR shifts were in high agreement with the experimental data (Table 2). The CMAE and CRMSE values were in the range of 1.09 to 1.87 ppm and 1.34 to 2.11 ppm, respectively. The ^{13}C results were obtained with excellent correlation coefficients ($r^2 \geq 0.9980$) for all 10 tested functionals. Compared to the results of ^{1}H shift calculations, the calculated ^{13}C data were more accurate due to the relatively smaller errors and stronger correlations of ^{13}C shifts. The noticeable deviations of carbon atoms **C4**, **C6** and **C10** were observed in the range of 1.18 to 3.94 ppm, 0.544 to 2.94 ppm, and 1.80 to 3.45 ppm, respectively (Figure 5). The three best functionals with low errors and high correlation coefficients were HSEH1PBE (CMAE = 1.19 ppm, CRMSE = 1.43 ppm, and r^2 = 0.9991), mPW1PW91 (CMAE = 1.14 ppm, CRMSE = 1.35 ppm, and r^2 = 0.9992), and ωB97XD (CMAE = 1.09 ppm, CRMSE = 1.34 ppm, and r^2 = 0.9992). These results

of ^{13}C chemical shift calculations would allow meaningful predictions with a high level of accuracy.

Table 2. The ^{13}C NMR chemical shifts of **1** calculated using 10 DFT functionals coupled with 6-31G(d,p) basis set in DMSO solvent. All chemical shifts, CMAEs, and CRMSEs are in ppm.

	^{13}C NMR Chemical shifts (**1**, DMSO)										Statistical parameters		
	C1	**C2**	**C3**	**C4**	**C5**	**C6**	**C7**	**C8**	**C9**	**C10**	CMAE	CRMSE	r^2
δ_{exp}	128.1	147.1	153.0	116.2	136.4	131.3	35.6	41.1	179.4	61.3			
B3LYP	129.9	148.6	153.1	113.5	136.9	129.8	37.2	42.7	179.6	58.0	1.48	1.76	0.9986
B3PW91	129.6	148.5	152.9	114.3	136.5	130.0	36.7	42.7	179.8	58.6	1.21	1.43	0.9991
BPV86	129.4	149.3	154.2	112.3	136.6	128.9	37.5	42.4	180.0	58.9	1.73	2.01	0.9982
CAMB3LYP	130.2	148.2	152.5	115.0	137.0	130.7	36.6	42.6	178.8	57.8	1.26	1.53	0.9989
HCTH	129.0	149.3	153.9	112.6	136.3	129.1	37.6	42.1	180.3	59.2	1.58	1.85	0.9985
HSEH1PBE*	**129.5**	**148.4**	**152.8**	**114.5**	**136.5**	**130.1**	**36.7**	**42.7**	**179.8**	**58.4**	**1.19**	**1.43**	**0.9991**
mPW1PW91*	**129.5**	**148.3**	**152.7**	**114.7**	**136.4**	**130.2**	**36.6**	**42.7**	**179.9**	**58.6**	**1.14**	**1.35**	**0.9992**
PBEPBE	129.4	149.3	154.2	112.5	136.6	129.0	37.6	42.3	179.9	58.8	1.69	1.95	0.9983
TPSSTPSS	128.8	149.5	153.8	112.3	135.7	128.3	37.5	42.7	181.4	59.5	1.87	2.11	0.9980
w*B97XD	**129.7**	**148.2**	**152.4**	**115.0**	**136.7**	**130.6**	**36.4**	**42.7**	**179.4**	**58.3**	**1.09**	**1.34**	**0.9992**

*The three functionals with lowest errors are in bold.

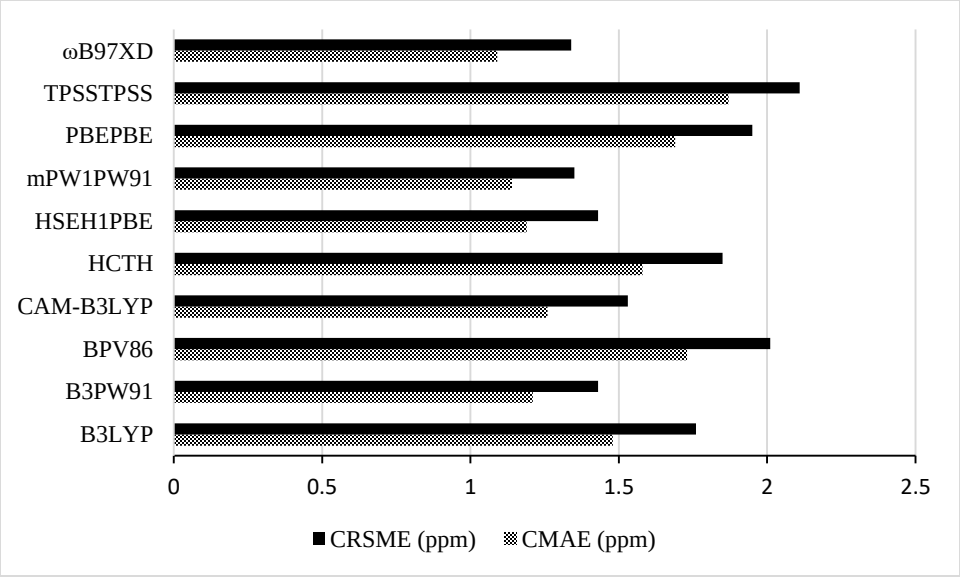

Figure 4. CMAE and CRSME values for the ^{13}C chemical shift calculations of dimer **1**

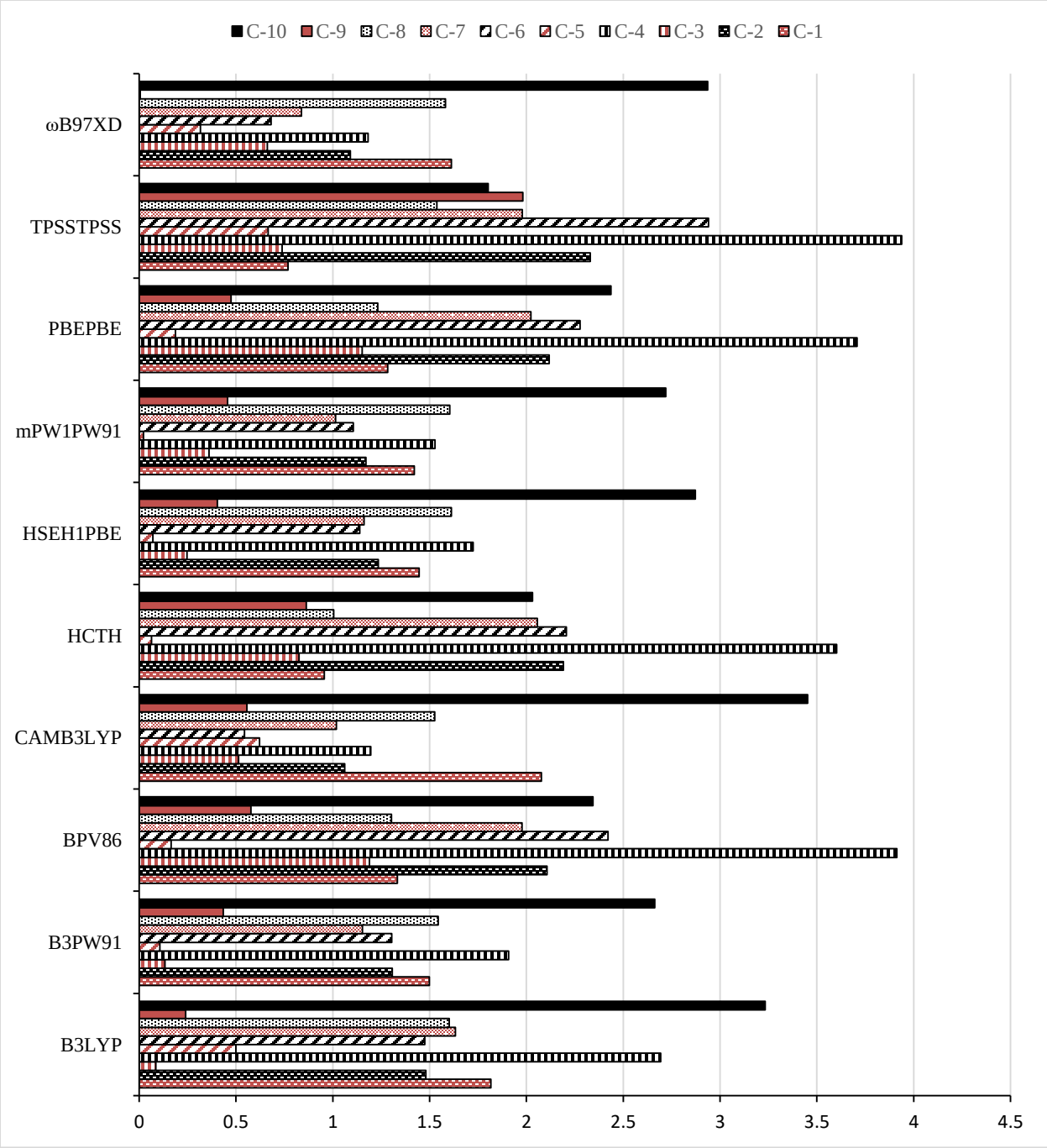

Figure 5. Absolute deviations of for the ^{1}H chemical shift calculations of dimer **1**

The evaluation of the selected functionals for lignin model dimers 2 and 3

HSEH1PBE, mPW1PW91, and *ω*B97XD functionals were employed for computing the ^{1}H and ^{13}C chemical shifts of lignin model dimers **2** and **3**. The above procedure of the theoretical calculations and statistical analysis of compound **1** was applied for compounds **2** and **3**. In general, the calculated results were observed with low associated errors and strong linear correlations ($r^2 \geq$ 0.9901). For the ^{1}H NMR shift calculations of **2** and **3**, the CMAE and CRMSE values were ranged

from 0.106 to 0.144 ppm and 0.124 to 0.168 ppm, respectively (Table 3). The largest deviations were found for atom **H6** of **2** ($|\Delta\delta|$ = 0.19 ppm) and atom **H4** of **3** ($|\Delta\delta|$ = 0.29 ppm). For the ^{13}C NMR shift calculations, the CMAE and CRMSE values in the ranges of 1.39 to 1.76 ppm and 1.58 to 2.01 ppm, respectively (Table 4). The noticeable deviations were observed for **C6** of **2** ($|\Delta\delta|$ = 2.83 ppm) and **C5** of **3** ($|\Delta\delta|$ = 3.01 ppm). Overall, the results of the performed calculations indicate that the selected functionals produced ^{1}H and ^{13}C chemical shifts with high accuracy.

Table 3. The calculated ^{1}H NMR chemical shifts of **2** and **3** in $CHCl_3$ using HSEH1PBE, mPW1PW91, and *ω*B97XD functionals coupled with 6-31G(d,p) basis set. All chemical shifts, CMAEs, and CRMSEs are in ppm.

	^{1}H NMR Chemical shifts (**2**)				Statistical parameters		
	H4	**H6**	**H7**	**H8**	CMAE	CRMSE	r^2
δ_{exp}	6.71	6.82	2.31	3.98			
HSEH1PBE	6.55	7.00	2.36	3.91	0.116	0.128	0.9955
Mpw1pw91	6.55	7.01	2.37	3.90	0.121	0.132	0.9952
*w*B97XD	6.56	7.00	2.36	3.91	0.112	0.124	0.9958

	^{1}H NMR Chemical shifts (**3**)						Statistical parameters		
	H4	**H6**	**H7**	**H8**	**H9**	**H10**	CMAE	CRMSE	r^2
δ_{exp}	6.73	6.76	3.38	5.99	5.11	3.92			
HSEH1PBE	6.51	6.76	3.36	6.03	5.28	3.83	0.107	0.128	0.9906
Mpw1pw91	6.51	6.88	3.37	6.02	5.28	3.83	0.106	0.128	0.9905
*w*B97XD	6.44	6.77	3.21	5.90	5.22	3.73	0.144	0.168	0.9901

Table 4. The calculated ^{13}C NMR chemical shifts of **2** and **3** in $CHCl_3$ using HSEH1PBE, mPW1PW91, and *ω*B97XD functionals coupled with 6-31G(d,p) basis set. All chemical shifts, CMAEs, and CRMSEs are in ppm.

	^{13}C NMR Chemical shifts (**2**)								Statistical parameters		
	C1	**C2**	**C3**	**C4**	**C5**	**C6**	**C7**	**C8**	CMAE	CRMSE	r^2
δ_{exp}	124.4	140.4	147.2	111.3	129.7	123.5	21.0	56.0			
HSEH1PBE	124.3	142.3	146.8	109.1	128.1	126.1	22.2	54.8	1.19	1.43	0.9991
mPW1PW91	124.2	142.3	146.7	109.2	128.1	126.1	22.1	54.8	1.14	1.35	0.9992
*w*B97XD	124.4	142.1	146.2	109.5	128.2	126.4	22.1	54.7	1.09	1.34	0.9992

	^{13}C NMR Chemical shifts (**3**)										Statistical parameters		
	C1	**C2**	**C3**	**C4**	**C5**	**C6**	**C7**	**C8**	**C9**	**C10**	CMAE	CRMSE	r^2
δ_{exp}	123.5	141.3	147.6	111.0	132.3	124.8	40.3	137.8	116.0	56.4			
HSEH1PBE	123.9	142.7	146.8	108.7	129.3	125.6	43.0	140.6	116.6	53.7	1.76	1.76	0.9966
mPW1PW91	123.9	142.7	146.7	108.9	129.4	125.6	42.8	140.4	116.7	53.9	1.68	1.68	0.9969
*w*B97XD	124.1	142.5	146.5	109.3	129.6	126.0	42.4	140.0	116.6	54.1	1.57	1.72	0.9975

4. Conclusion

We have performed the evaluation of 10 DFT functionals coupled with 6-31G(d,p) basis set using GIAO method and IEFPCM model on the calculation of ^1H and ^{13}C chemical shifts of 5-5 dimer **1**, which was effectively synthesized from ferulic acid in 72% yield over two steps. Our results showed the three best performing functionals for the ^1H and ^{13}C shift calculation were HSEH1PBE, mPW1PW91, and *ω*B97XD with CMAEs ≤ 0.0611 ppm and CRMSEs ≤ 0.0650 ppm for ^1H and CMAEs ≤ 1.19 ppm and CRMSEs ≤ 1.43 ppm for ^{13}C. In these cases, excellent correlations between theoretical and experimental data ($r^2 > 0.9988$) were observed. The calculations of ^1H and ^{13}C chemical shifts of two other lignin model dimers **2** and **3** using the best performing functionals also produced good accuracy results with CMAEs ≤ 0.144 ppm for ^1H and CMAEs ≤ 1.76 ppm for ^{13}C. The computed ^1H and ^{13}C shifts were well correlated with the experimental data ($r^2 > 0.9901$). Overall, the method *ω*B97XD/6-31G(d,p)/IEFPCM consistently provided the calculated ^1H and ^{13}C chemical shifts with a high level of accuracy. Given such high degree of accuracy achieved in calculating the ^1H and ^{13}C chemical shifts of 5-5 lignin model dimer **1**, **2**, and **3**, the results of this work can be used for supporting the assignments of the experimental NMR spectra of the 5-5 dimer substructures of lignin polymers and further studies on the chemical shift calculations of other lignin model dimers and similar biaryl systems are under investigation.

Experimental

Experimental measurements were carried out at University of Helsinki. ^{1}H and ^{13}C NMR spectra were recorded on a Varian 300 MHz spectrometer at ambient temperature. ^{1}H and ^{13}C chemical shifts are reported in ppm using residual solvent peaks as an internal reference (DMSO: 2.50 ppm for ^{1}H NMR and 37.52 ppm for ^{13}C NMR). The MS spectrum of **1** was obtained using University of Helsinki's mass spectrometric facility on Micromass Autospec Ultima instrument via CI method.

Synthesis of 1

***3,3'-(6,6'-dihydroxy-5,5'-dimethoxy-[1,1'-biphenyl]-3,3'-diyl)dipropionic acid* (1).** A solution of ferulic acid (3.4 g, 17.5 mmol) in 50 ml ethanol containing 10% Pd/C (0.50 g) was hydrogenated for 2h at room temperature. After filtrating off the catalyst, the solvent was evaporated to give a yellow solid (3.4 g). To a solution of this yellow solid and NaOH (2.82 g, 70.5 mmol) in H_2O, a solution of I_2 (5.44g, 21.4 mmol) and KI (3.5 g, 21.1 mmol) was added dropwise and the mixture was stirred overnight at room temperature. An aqueous solution of $Na_2S_2O_3$ was added to the mixture to remove residual I_2. The mixture was then acidified by HCl solution to pH = 2 after which it was filtered and washed with H_2O to yield a white solid; **^{1}H-NMR** (300 MHz, DMSO): δ (ppm) 6.78 (d, *J* = 1.8 Hz, 2H), 6.56 (m, *J* = 2.1 Hz, 2H), 3.79 (s, 6H), 2.74 (m, 4H), 2.49 (m, 4H); **^{13}C-NMR** (75 MHz, DMSO): δ (ppm) 179.4, 153.0, 147.1, 136.4, 131.3, 128.1, 116.2, 61.3, 41.1, 35.6. Molecular ion: $[M-H]^+$ 389

5. Acknowledgements

T. T. N. would like to thank the Erasmus Mundus Scholarship (2009-2011) for the financial support.

References

[1] A.J. Ragauskas, G.T. Beckham, M.J. Biddy, R. Chandra, F. Chen, M.F. Davis, B.H. Davison, R.A. Dixon, P. Gilna, M. Keller, P. Langan, A.K. Naskar, J.N. Saddler, T.J. Tschaplinski, G.A. Tuskan, C.E. Wyman, Lignin valorization: Improving lignin processing in the biorefinery, Science (80-.). 344 (2014) 1246843. https://doi.org/10.1126/science.1246843.

[2] W. Boerjan, J. Ralph, M. Baucher, Lignin Biosynthesis, Annu. Rev. Plant Biol. 54 (2003) 519–546. https://doi.org/10.1146/annurev.arplant.54.031902.134938.

[3] P. Oyarce, B. De Meester, F. Fonseca, L. de Vries, G. Goeminne, A. Pallidis, R. De Rycke, Y. Tsuji, Y. Li, S. Van den Bosch, B. Sels, J. Ralph, R. Vanholme, W. Boerjan, Introducing curcumin biosynthesis in Arabidopsis enhances lignocellulosic biomass processing, Nat. Plants. 5 (2019) 225–237. https://doi.org/10.1038/s41477-018-0350-3.

[4] G.A. Tuskan, The unexpected malleability of lignin, Nat. Plants. 5 (2019) 128. https://doi.org/10.1038/s41477-019-0360-9.

[5] T. Nakamura, H. Kawamoto, S. Saka, Pyrolysis behavior of Japanese cedar wood lignin studied with various model dimers, J. Anal. Appl. Pyrolysis. 81 (2008) 173–182. https://doi.org/10.1016/j.jaap.2007.11.002.

[6] L. Caramelo, M.J. Martínez, Á.T. Martínez, A search for ligninolytic peroxidases in the Fungus pleurotus eryngii involving α-keto-γ-thiomethylbutyric acid and lignin model dimers, Appl. Environ. Microbiol. 65 (1999) 916–922. https://doi.org/10.1128/aem.65.3.916-922.1999.

[7] J. Pellinen, E. Väisänen, M. Salkinoja-Salonen, G. Brunow, Utilization of dimeric lignin model compounds by mixed bacterial cultures, Appl. Microbiol. Biotechnol. 20 (1984) 77–82. https://doi.org/10.1007/BF00254650.
[8] H. Wariishi, K. Valli, M.H. Gold, Oxidative Cleavage of a Phenolic Diarylpropane Lignin Model Dimer by Manganese Peroxidase from Phanerochaete chrysosporium, Biochemistry. 28 (1989) 6017–6023. https://doi.org/10.1021/bi00440a044.
[9] A.L. Jongerius, R. Jastrzebski, P.C.A. Bruijnincx, B.M. Weckhuysen, CoMo sulfide-catalyzed hydrodeoxygenation of lignin model compounds: An extended reaction network for the conversion of monomeric and dimeric substrates, J. Catal. 285 (2012) 315–323. https://doi.org/10.1016/j.jcat.2011.10.006.
[10] B. Güvenatam, O. Kurşun, E.H.J. Heeres, E.A. Pidko, E.J.M. Hensen, Hydrodeoxygenation of mono- and dimeric lignin model compounds on noble metal catalysts, Catal. Today. 233 (2014) 83–91. https://doi.org/10.1016/j.cattod.2013.12.011.
[11] H.D. Watts, M.N.A. Mohamed, J.D. Kubicki, Comparison of multistandard and TMS-standard calculated NMR shifts for coniferyl alcohol and application of the multistandard method to lignin dimers, J. Phys. Chem. B. 115 (2011) 1958–1970. https://doi.org/10.1021/jp110330q.
[12] J.S. Lomas, ^{1}H NMR spectra of alcohols and diols in chloroform: DFT/GIAO calculation of chemical shifts, Magn. Reson. Chem. 52 (2014) 745–754. https://doi.org/10.1002/mrc.4130.
[13] B.G. Diehl, H.D. Watts, J.D. Kubicki, M.R. Regner, J. Ralph, N.R. Brown, Towards lignin-protein crosslinking: Amino acid adducts of a lignin model quinone methide, Cellulose. 21 (2014) 1395–1407. https://doi.org/10.1007/s10570-014-0181-y.
[14] K. Wolinski, J.F. Hinton, P. Pulay, Efficient Implementation of the Gauge-Independent Atomic Orbital Method for NMR Chemical Shift Calculations, J. Am. Chem. Soc. 112 (1990) 8251–8260. https://doi.org/10.1021/ja00179a005.
[15] J. Gauss, Effects of electron correlation in the calculation of nuclear magnetic resonance chemical shifts, J. Chem. Phys. 99 (1993) 3629–3643. https://doi.org/10.1063/1.466161.
[16] R. Ditchfield, Self-consistent perturbation theory of diamagnetism I. A gauge-invariant LCAO method for N.M.R. Chemical shifts, Mol. Phys. 27 (1974) 789–807. https://doi.org/10.1080/00268977400100711.
[17] M.A. Iron, Evaluation of the Factors Impacting the Accuracy of 13C NMR Chemical Shift Predictions using Density Functional Theory - The Advantage of Long-Range Corrected Functionals, J. Chem. Theory Comput. 13 (2017) 5798–5819. https://doi.org/10.1021/acs.jctc.7b00772.
[18] S.A. Ralph, J. Ralph,, L.L. Landucci, NMR Database of Lignin and Cell Wall Model Compounds, Http://Ars.Usda.Gov/Services/ Docs.Htm?Docid=10491. (2004).
[19] A.D. Becke, Density-functional thermochemistry. III. The role of exact exchange, J. Chem. Phys. 98 (1993) 5648–5652. https://doi.org/10.1063/1.464913.
[20] A.D. Becke, Density-functional exchange-energy approximation with correct asymptotic behavior, Phys. Rev. A. 38 (1988) 3098–3100. https://doi.org/10.1103/PhysRevA.38.3098.
[21] C. Lee, W. Yang, R.G. Parr, Development of the Colle-Salvetti correlation-energy formula into a functional of the electron density, Phys. Rev. B. 37 (1988) 785–789. https://doi.org/10.1103/PhysRevB.37.785.
[22] P.J. Stephens, F.J. Devlin, C.F. Chabalowski, M.J. Frisch, Ab Initio calculation of

vibrational absorption and circular dichroism spectra using density functional force fields, J. Phys. Chem. 98 (1994) 11623–11627. https://doi.org/10.1021/j100096a001.
[23] J.P. Perdew, J.A. Chevary, S.H. Vosko, K.A. Jackson, M.R. Pederson, D.J. Singh, C. Fiolhais, Atoms, molecules, solids, and surfaces: Applications of the generalized gradient approximation for exchange and correlation, Phys. Rev. B. 46 (1992) 6671–6687. https://doi.org/10.1103/PhysRevB.46.6671.
[24] J.P. Perdew, J.A. Chevary, S.H. Vosko, K.A. Jackson, M.R. Pederson, D.J. Singh, C. Fiolhais, Erratum: Atoms, molecules, solids, and surfaces: Applications of the generalized gradient approximation for exchange and correlation (Physical Review B (1993) 48, 7, (4978)), Phys. Rev. B. 48 (1993) 4978. https://doi.org/10.1103/PhysRevB.48.4978.2.
[25] J.P. Perdew, Density-functional approximation for the correlation energy of the inhomogeneous electron gas, Phys. Rev. B. 33 (1986) 8822–8824. https://doi.org/10.1103/PhysRevB.33.8822.
[26] S.H. Vosko, L. Wilk, M. Nusair, Accurate spin-dependent electron liquid correlation energies for local spin density calculations: a critical analysis, Can. J. Phys. 58 (1980) 1200–1211. https://doi.org/10.1139/p80-159.
[27] T. Yanai, D.P. Tew, N.C. Handy, A new hybrid exchange-correlation functional using the Coulomb-attenuating method (CAM-B3LYP), Chem. Phys. Lett. 393 (2004) 51–57. https://doi.org/10.1016/j.cplett.2004.06.011.
[28] F.A. Hamprecht, A.J. Cohen, D.J. Tozer, N.C. Handy, Development and assessment of new exchange-correlation functionals, J. Chem. Phys. 109 (1998) 6264–6271. https://doi.org/10.1063/1.477267.
[29] A. Daniel Boese, N.L. Doltsinis, N.C. Handy, M. Sprik, New generalized gradient approximation functionals, J. Chem. Phys. 112 (2000) 1670–1678. https://doi.org/10.1063/1.480732.
[30] A.D. Boese, N.C. Handy, A new parametrization of exchange-correlation generalized gradient approximation functionals, J. Chem. Phys. 114 (2001) 5497–5503. https://doi.org/10.1063/1.1347371.
[31] J. Heyd, G.E. Scuseria, M. Ernzerhof, Hybrid functionals based on a screened Coulomb potential, J. Chem. Phys. 118 (2003) 8207–8215. https://doi.org/10.1063/1.1564060.
[32] M. Ernzerhof, J.P. Perdew, Generalized gradient approximation to the angle- and system-averaged exchange hole, J. Chem. Phys. 109 (1998) 3313–3320. https://doi.org/10.1063/1.476928.
[33] J.P. Perdew, K. Burke, Generalized gradient approximation for the exchange-correlation hole of a many-electron system, Phys. Rev. B - Condens. Matter Mater. Phys. 54 (1996) 16533–16539. https://doi.org/10.1103/PhysRevB.54.16533.
[34] C. Adamo, V. Barone, Exchange functionals with improved long-range behavior and adiabatic connection methods without adjustable parameters: The mPW and mPW1PW models, J. Chem. Phys. 108 (1998) 664–675. https://doi.org/10.1063/1.475428.
[35] J.P. Perdew, K. Burke, M. Ernzerhof, Generalized gradient approximation made simple, Phys. Rev. Lett. 77 (1996) 3865–3868. https://doi.org/10.1103/PhysRevLett.77.3865.
[36] J. Tao, J.P. Perdew, V.N. Staroverov, G.E. Scuseria, Climbing the density functional ladder: Nonempirical meta–generalized gradient approximation designed for molecules and solids, Phys. Rev. Lett. 91 (2003) 146401. https://doi.org/10.1103/PhysRevLett.91.146401.
[37] J.P. Perdew, A. Ruzsinszky, G.I. Csonka, L.A. Constantin, J. Sun, Workhorse semilocal

density functional for condensed matter physics and quantum chemistry, Phys. Rev. Lett. 103 (2009) 026403. https://doi.org/10.1103/PhysRevLett.103.026403.
[38] J. Da Chai, M. Head-Gordon, Systematic optimization of long-range corrected hybrid density functionals, J. Chem. Phys. 128 (2008) 084106. https://doi.org/10.1063/1.2834918.
[39] J. Chai, M. Head-Gordon, Long-range corrected hybrid density functionals with damped atom–atom dispersion corrections, Phys. Chem. Chem. Phys. 10 (2008) 6615–6620. https://doi.org/10.1039/B810189B.
[40] M.M. Francl, W.J. Pietro, W.J. Hehre, J.S. Binkley, M.S. Gordon, D.J. DeFrees, J.A. Pople, Self-consistent molecular orbital methods. XXIII. A polarization-type basis set for second-row elements, J. Chem. Phys. 77 (1982) 3654–3665. https://doi.org/10.1063/1.444267.
[41] M.J. Frisch, J.R. Cheeseman, G. Scalmani, V. Barone, B. Mennucci, G.A. Petersson, H. Nakatsuji, M. Caricato, X. Li, H.P. Hratchian, A.F. Izmaylov, J. Bloino, G. Zheng, J.L. Sonnenberg, M. Hada, M. Ehara, K. Toyota, R. Fukuda, J. Hasegawa, M. Ishida, T. Nakajima, Y. Honda, O. Kitao, H. Nakai, T. Vreven, J.A. Montgomery Jr., J.E. Peralta, F. Ogliaro, M. Bearpark, J.J. Heyd, E. Brothers, K.N. Kudin, V.N. Staroverov, T. Keith, R. Kobayashi, J. Normand, K. Raghavachari, A. Rendell, J.C. Burant, S.S. Iyengar, J. Tomasi, M. Cossi, N. Rega, J.M. Millam, M. Klene, J.E. Knox, J.B. Cross, V. Bakken, C. Adamo, J. Jaramillo, R. Gomperts, R.E. Stratmann, O. Yazyev, A.J. Austin, R. Cammi, C. Pomelli, J.W. Ochterski, R.L. Martin, K. Morokuma, V.G. Zakrzewski, G.A. Voth, P. Salvador, J.J. Dannenberg, S. Dapprich, A.D. Daniels, O. Farkas, J.B. Foresman, J. V. Ortiz, J. Cioslowski, F.D. J., Gaussian 09, Revision D.01, (2013).
[42] J. Tomasi, B. Mennucci, R. Cammi, Quantum mechanical continuum solvation models, Chem. Rev. 105 (2005) 2999–3093. https://doi.org/10.1021/cr9904009.
[43] J. Tomasi, B. Mennucci, E. Cancès, The IEF version of the PCM solvation method: An overview of a new method addressed to study molecular solutes at the QM ab initio level, in: J. Mol. Struct. THEOCHEM, Elsevier, 1999: pp. 211–226. https://doi.org/10.1016/S0166-1280(98)00553-3.
[44] F.A. Marques, F. Simonelli, A.R.M. Oliveira, G.L. Gohr, P.C. Leal, Oxidative coupling of 4-substituted 2-methoxy phenols using methyltributylammonium permanganate in dichloromethane, Tetrahedron Lett. 39 (1998) 943–946. https://doi.org/10.1016/S0040-4039(97)10665-7.
[45] M. Albrecht, M. Schneider, The preparation of rigid linear Di- (and Tri-)catechol derivatives, Synthesis (Stuttg). 2000 (2000) 1557–1560. https://doi.org/10.1055/s-2000-7604.
[46] N. Kumar, N. Yadav, N. Amarnath, V. Sharma, S. Shukla, A. Srivastava, P. Prasad, A. Kumar, S. Garg, S. Singh, S. Sehrawat, B. Lochab, Integrative natural medicine inspired graphene nanovehicle-benzoxazine derivatives as potent therapy for cancer, Mol. Cell. Biochem. 454 (2019) 123–138. https://doi.org/10.1007/s11010-018-3458-x.
[47] R. Bortolomeazzi, G. Verardo, A. Liessi, A. Callea, Formation of dehydrodiisoeugenol and dehydrodieugenol from the reaction of isoeugenol and eugenol with DPPH radical and their role in the radical scavenging activity, Food Chem. 118 (2010) 256–265. https://doi.org/10.1016/j.foodchem.2009.04.115.